Luminescence of Cr^{3+} in sillimanite

A. J. Wojtowicz* and A. Lempicki
Department of Chemistry, Boston University, 590 Commonwealth Avenue, Boston, Massachusetts 02215
(Received 20 May 1988)

The broadband luminescence peaking at about 790 nm in a natural sample of sillimanite was investigated. The origin of luminescence is most likely Cr impurities. The temperature dependences of decay time, total intensity, and thermal broadening of emission line shapes were measured. Relatively long decay times at room temperature (~ 160 μs), thermal stimulation of radiative transition rates, and relatively slow nonradiative rates were observed. The unusually small value of the frequency factor ($\sim 10^6$) standing in sharp contrast to other Cr-doped materials indicates the forbidden nature of the nonradiative transition. The room-temperature quantum efficiency was estimated to be about 80%. The material shows promise for successful laser applications.

I. INTRODUCTION

This paper describes unusual properties of Cr^{3+} luminescence in a natural crystal of sillimanite. As will be seen this host presents one of the lowest crystal fields encountered in oxides and the longest reported decay time. In addition preliminary results indicate that mechanisms responsible for nonradiative decay rates elude presently advanced modes of nonradiative deactivation.[1-5] The inversion symmetry of Cr site (Cr substituting for Al), accounts presumably for the relatively long radiative $^4T_2$ lifetime, while the small value of the so-called frequency factor expressing the promoting mode matrix element, indicates the forbidden nature of the nonradiative transition. Subject to determining problems connected with crystal growth, this material may prove to be of great interest for tunable solid-state lasers.

Sillimanite is one of the three well-known polymorphs of the alluminosilicate Al_2SiO_5, the others being kyanite and andalusite. Our interest in these materials stems from the fact that sillimanite, whose chemical formula can be expressed as $Al_2O_3 \cdot SiO_2$, is the parent of the crystalline phase known as mullite ($Al_2[Al_{2+2x}Si_{2-2x}]O_{10-x}$) which precipitates in Cr-doped glass ceramics extensively studied by us.[6,7] While there exists a close similarity between the crystal structure of mullites and sillimanite,[8,9] the former are characterized by a built-in disorder due to the presence of oxygen vacancies. This disorder causing large inhomogeneous broadening of absorption and emission lines of Cr^{3+}, observed in mullite ceramics, is absent in sillimanite making it a crystaline host of great potential interest for tunable solid-state laser applications.

The paper is organized as follows. In Sec. II a brief description of the material and experimental techniques is given. In Sec. III results are reported including luminescence spectra, decays, and total intensity measurements versus temperature. In Sec. IV the one-configuration-coordinate model of Cr luminescence center is constructed using spectral data. Eventually in Sec. V conclusions are presented.

II. EXPERIMENT

A. Material

Sillimanite has an orthorhombic symmetry with a space group *Pbnm*. The lattice constants are $a=7.4883$ Å, $b=7.6808$ Å, $c=5.7774$ Å. It has a good cleavage along [010]. A hardness of the crystal is about 6.5–7.5, density is 3.2386 g/cm^3. It has optically positive character with $\alpha=1.654-1.661$, $\beta=1.658-1.662$, $\gamma=1.673-1.683$. Principal strain components of thermal expansion per 1 °C are 0.66×10^{-5} 0.40×10^{-5}, and 0.16×10^{-5}.[10] The structure contains edge-sharing, strictly centrosymmetric octahedra (Al sites) arranged in straight chains parallel to [001] and alternating corner-sharing tetrahedra (Al and Si sites). Due to the large stabilization energy octahedra are preferred sites for Cr^{3+}.

A natural specimen of sillimanite obtained from the Museum of Natural History of the Smithsonian Institution (sample designation R3732), was analyzed by x-ray fluorescence for the presence of trace transition-metal elements.[11] The dominant impurities were found to be Fe, Ti, and Cr. The sample was not of sufficient quality to perform absorption measurements, therefore all of our conclusions were made on the basis of emission spectroscopy and lifetimes as a function of temperature between 27 and 600 K.

B. Techniques

The experimental arrangement consisted of a $\frac{1}{2}m$ Jarrell-Ash spectrometer, RCA C31034A (GaAs) or ITT FW118 (S-1) dry-ice-cooled photomultiplier tubes, combination of Keithley 427 current amplifier, and Kinetic Systems 3552 analog-to-digital (A/D) converter or DSP Technologies 2001 transient recorder, Coherent Innova 20 Ar-ion laser (200 mW, 514.5 nm), or Lambda-Physik FL 2000 pulsed dye laser (Exciton Rhodamine-610), used for steady-state or time-resolved experiments, respectively. The experiment was controlled by the Kinetic Systems camac and ITT XTRA/286 ATW personal comput-

er where data were stored for subsequent analysis. The emission spectra were corrected for spectral response of the system using a standard lamp. Variable temperature was obtained by use of the Cryosystems LTS-22-Hi-Temp closed-cycle helium refrigerator.

III. RESULTS

For the purpose of quantitative analysis of luminescence spectra we perform a transformation from intensities as measured by the photomultiplier to line shapes. This is accomplished by first correcting the intensities (in wavelength scale) for the spectral response of the detecting system and then dividing by the sixth power of frequency.[7] The line shapes (in energy scale) of the emission band of sillimanite excited by a cw Ar ion laser at 514.5 nm, are given in Fig. 1 for two temperatures. The nearly featureless, bell-shaped curves, centered at approximately 12 000 cm^{-1} are strongly reminiscent of the emission of Cr^{3+} situated in low crystal-field environment ($^4T_2$-$^4A_2$ transition).[12] In view of the detected presence of Fe and Ti in the sample we cannot immediately rule out Fe^{3+} or Ti^{3+} as the possible origins of this band. Fe^{3+} in octahedral sites emits at longer wavelengths but in tetrahedral sites could well be mistaken for Cr^{3+} in low fields.[13,14] However in Fe^{3+} at both high and low fields ($^4T_1$ to $^6A_1$ or $^2T_2$), the transitions are spin forbidden and the lifetimes are invariably in the millisecond range. As seen from Fig. 2 the decays observed in sillimanite are exponential and the decay time is about 160 μs at room temperature. It is constant across the whole emission band and at 27 K increases to 260 μs. This rules out Fe as the emitting species.

Correspondingly Ti^{3+} in octahedral sites, whose emission is spin allowed, could well have an emission in the near-ir (infrared) region. However, in this case the decay times, even in sites possessing inversion symmetry are characteristically short.[15] On the other hand the decay times of the $^4T_2$-$^4A_2$ transitions in Cr^{3+} situated in centrosymmetric sites are known to lie in the range observed by us.[16,17] We feel therefore that the assignment of the emission to Cr^{3+} is unambiguous.

The temperature dependence of the integrated intensity (in arbitrary inverse-time units) is given in Fig. 3. The solid curve drawn through the points (○) corresponds to the traditionally simplest model of nonradiative decay for strongly coupled systems (to be discussed in more detail in Sec. IV):

$$I=\frac{W}{1+\tau_r s \exp(-E/kT)} . \quad (1)$$

In this formula W is the pumping rate (in units of s^{-1}), τ_r is the radiative lifetime, E is the activation energy, and s is the frequency factor. The least-squares linear regression fit of expression (1) to experimental points gives $s=(3.6\pm0.9)\times10^6$ s^{-1}, and $E=(1700\pm100)$ cm^{-1}. We estimate that the quantum efficiency at 300 K is about 80%. On the same figure we also show points (×) corresponding to the measured decay times. They generally show the same trend but with a difference. While the integrated intensity does not decrease significantly up to 250 K, the decay time shows a downward trend starting at about 100 K. It is important to ascertain that this difference is not a result of a systematic error. To avoid a temperature reading error due to the poor thermal contact between sample and cold (or hot) finger the measurements were taken with both decreasing and increasing temperature. The differences were insignificant. Another potential source of error could be due to a difference in the true local temperature of the sample, due to the different methods of excitation. The spectra were taken with a cw Ar laser operating at 200 mW, while for the decays a pulsed dye laser of approximately 2 mW of average power was used. One could argue that the local temperature in the case of the cw excitation is higher than measured by the finger sensor. If this were true, the correct integrated intensity curve should be displaced more to the right, thus accentuating rather than diminishing the difference between the decay and the intensity curves. The "hysteresis" between the two curves appears therefore to be a genuine phenomenon to which we shall come

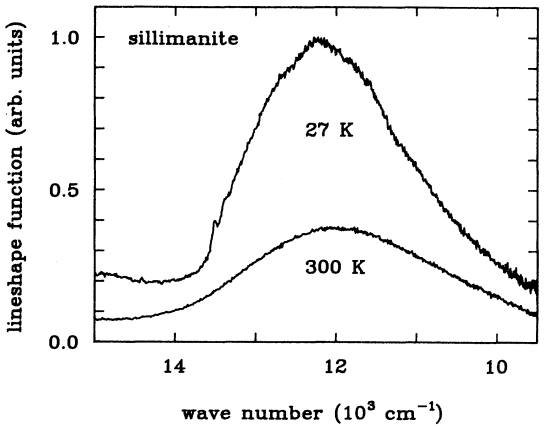

FIG. 1. Sillimanite luminescence. The line-shape functions calculated from corrected luminescence spectra are shown for 27 and 300 K.

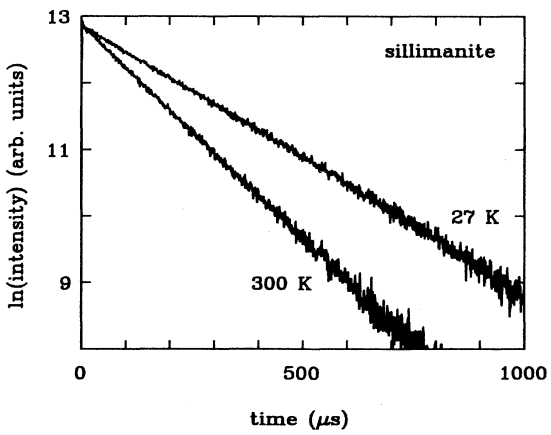

FIG. 2. Sillimanite luminescence decays for 27 and 300 K.

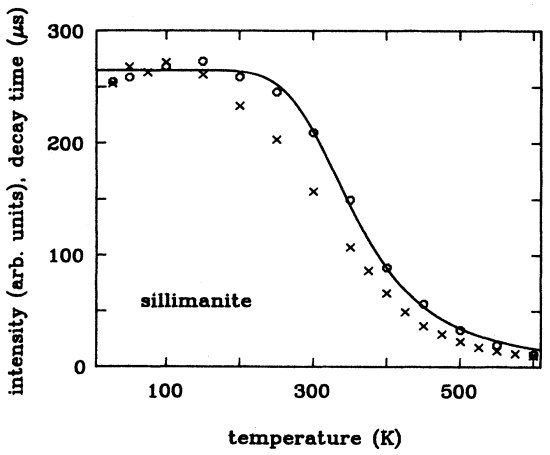

FIG. 3. The temperature dependence of total intensity and decay times. ○, total intensity, experimental points; ×, decay times, experimental points; solid curve, temperature dependence of total intensity, theory.

back later. The similar phenomenon was observed before[5,16,18] and was interpreted in terms of the Liehr-Balhausen model.[19,5]

Figure 4 is a plot of a second moment of the emission line-shape function versus temperature. Simple theory assuming linear coupling to a single mode relates this moment to the temperature by the expression:[20]

$$\langle \sigma \rangle = S(\hbar\omega)^2 \coth(\hbar\omega/2kT) , \quad (2)$$

where S is the Huang-Rhys coupling constant and ω is the phonon frequency. We see that except at the highest temperatures the theoretical fit is quite satisfactory. The deviation observed at higher temperatures may be due to the nonlinear coupling to low-energy lattice (or resonance) modes.[21] The best fit was obtained for $S=7.3$ and $\hbar\omega=363\ \text{cm}^{-1}$.

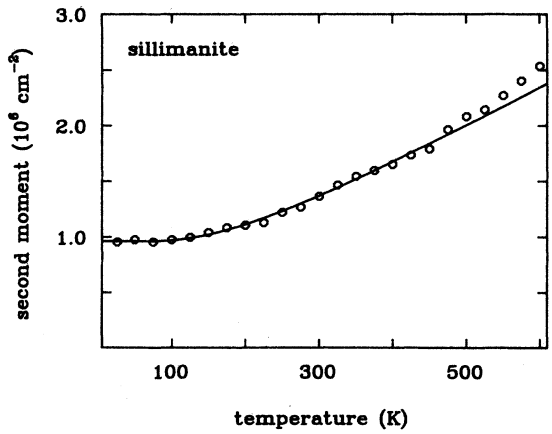

FIG. 4. Temperature dependence of the second moment of sillimanite luminescence line-shape function. ○, experimental points; solid curve, theory.

IV. DISCUSSION

A. Emission spectra

As mentioned previously the general appearance of the emission spectrum resembles that of the low-field Cr. We can state that without the knowledge of absorption spectrum and consequently the explicit value of the crystal-field parameter Dq. Low-field spectra typically show only a broadband due to $^4T_2$-$^4A_2$ transition without the sharp R line due to the ^2E-$^4A_2$ transition. This occurs whenever the minimum of the configuration coordinate parabola for $^4T_2$ falls below the minimum of the ^2E parabola. In this case the energy difference between the two minima (d) is negative. Well-documented examples of such low-field spectra occur in glasses,[22] in elpasolites,[16] in gadolinium scandium gallium garnets (GSGG), gadolinium gallium garnets (GGG), and lanthanum lutetium gallium garnets (LLGG),[23] in La silicate,[24] as well as in scandium borate.[18] Table I gives the position of the emission maximum, the room-temperature decay times, and the parameter d. We see that sillimanite fits well into that category of materials.

The next item of interest is the origin of the small, but perfectly reproducible line at 694 nm (14 409 cm^{-1}) observed at low temperatures (Fig. 5). The position of this line is disturbingly close to where one might expect the medium insensitive, R line, to be. Should this be indeed an R line, our strict classification of sillimanite as a low-field material ($d<0$) would not be tenable. It is our contention that this is not an R line but rather a false origin of the broadband, $^4T_2$-$^4A_2$ emission. This conclusion is reached primarily on the basis of the temperature dependence of the 694-nm line shown in Fig. 6. We see that as the temperature is raised from 27 K the line persists with almost unchanged amplitude up to 200 K and then slowly dissolves at higher temperatures. The behavior of an R line should be quite different. If $d<0$ then at the lowest temperature there cannot be any R line due to the domineering effect of the quartet with its short (spin-allowed) lifetime. As the temperature is raised, there may be some activation of the ^2E level and the R line may start to appear. This is contrary to our observations. If $d>0$ then at the lowest temperature the ^2E level should freeze out most of the population and the R line would dominate. Depending on the value of d, higher temperatures will bring about the emergence of the broadband of the quartet as happens say in emerald or ruby. This too is contrary to observation and we have to conclude that in spite of the energy coincidence, the 694-nm line does not correspond to an R line. The alternative, which we support, is that it is a part of the quartet structure. The remaining false origins of the spin-orbit split quartet are either unpopulated or lost in the noise. Another remote possibility is that the 694-nm line is indeed an R line corresponding to an altogether different, less populous, high-field site. There is no crystallographic justification for this contention and its disappearance with increasing temperature does not make it probable. We therefore conclude that the 694-nm line is indeed a false origin of the quartet and plays a role of the zero-phonon line for broadband. Assuming this, the comparison of the areas

TABLE I. Summary of emission parameters of low-field, Cr-doped materials.

Host	Emission peak (nm)	Lifetime (μs)	d (cm^{-1})	Reference
$Gd_3Sc_2Ga_5O_{12}$(GSGG)	760	115	50	23
$Gd_3Ga_5O_{12}$(GGG)	740	160		23
$La_3Lu_5Ga_5O_{12}$(LLGG)	840	68	−1000	23
$ScBO_3$	810	115		18
$La_3Ga_5SiO_{14}$	890	5.3		24
K_2NaScF_6	765	285	−1000	12
K_2LiScF_6	750		−300	12
K_2NaAlF_6	740			12
K_2NaGaF_6	740	290		16
Cs_2NaYCl_6	1030	13		16
$Al(PO_3)_3$	78	124		12
Sillimanite	790	160	<0	this paper

under the line shapes of this line and broadband yields the total coupling coefficient as $S_{tot}=8.2$.

Following this line of interpretation it is interesting to examine the low-energy side of the 694-nm line, shown in Fig. 5. Although poorly resolved, it appears as a progression of a 340 cm^{-1} phonon. Two components of this progression can be resolved in the spectrum (the line at 670 cm^{-1} would be the second and that at 1020 cm^{-1} would be the third replicas of the zero-phonon line). The coupling constant for this mode is clearly much higher than 1 and from the intensity ratios can be roughly estimated to be in the range 3–6. Additionally a second mode about 890 cm^{-1} can be resolved. Unfortunately, it is evident that we are dealing here with a multiphonon sideband and that identification as well as an extraction of the single-phonon frequencies may be very much in error.

However, it is important to note that the 340-cm^{-1} phonon energy is quite close to that found from the temperature broadening of luminescence line shapes (360 cm^{-1}, see Sec. III) although it is somewhat smaller. This can be rationalized in terms of an "effective" phonon energy contributing to the broadening of the spectrum with the temperature. The higher effective value comes from the contribution of higher-energy modes, the likely candidate being the relatively weakly coupled 890-cm^{-1} mode resolved in the luminescence spectrum. Also an estimation of the coupling constant from these two experiments is in reasonable agreement. Since this coupling constant (most likely 6–7) is only somewhat smaller than the total coupling constant ($S_{tot}=8.2$) we conclude that the 340-cm^{-1} mode is likely to be an a_{1g} full symmetry breathing mode.

B. Thermal quenching

We now come to a most significant and least controversial conclusion which concerns the quenching of the decay time and the total intensity with temperature. These data can be used to check consistency of the model of the Cr^{3+} luminescence center deduced from spectral data. The total intensity temperature dependence in the two-level system for steady state results from

$$W=\frac{n}{\tau_r}+\frac{n}{\tau_{nr}} \tag{3}$$

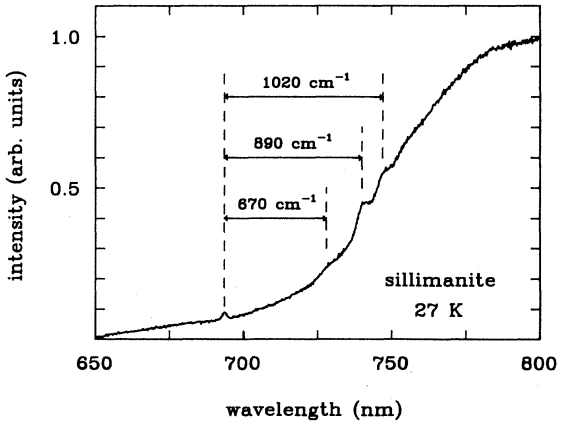

FIG. 5. Sillimanite luminescence spectrum, uncorrected. The structured, high-energy side of the band is shown. Temperature 27 K.

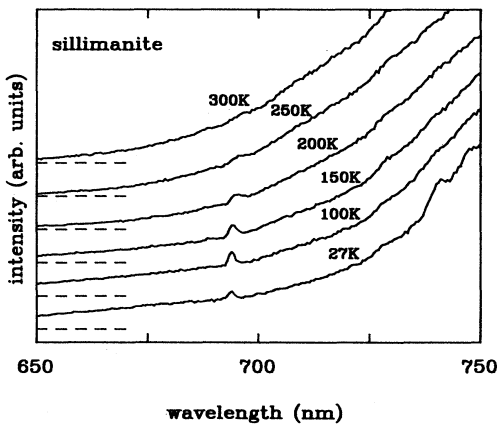

FIG. 6. High-energy side of sillimanite luminescence band for different temperatures, uncorrected. Dashed lines give baselines for consecutive spectra.

and

$$I=\frac{n}{\tau_r}\ , \tag{4}$$

where n is the population of the upper level, W and I are pumping rate and luminescence intensity in units proportional to photons/s, and τ_r, τ_{nr} are radiative and nonradiative lifetimes, respectively.

From (3) and (4) it follows immediately that

$$I=\frac{W}{1+\tau_r/\tau_{nr}} \tag{5}$$

and assuming Mott-type expression for $1/\tau_{nr}$,[25]

$$\frac{1}{\tau_{nr}}=s\exp(-E/kT)\ , \tag{6}$$

to be discussed more fully later, we have[26]

$$I=\frac{W}{1+\tau_r s\exp(-E/kT)} \tag{7}$$

which is the formula used to find E and s as described in Sec. III. Now, since

$$\frac{1}{\tau_{tot}}=\frac{1}{\tau_r}+\frac{1}{\tau_{nr}} \tag{8}$$

the temperature dependence of τ_{tot} using (6) can be found to be[26]

$$\tau_{tot}=\frac{\tau_r}{1+\tau_r s\exp(-E/kT)}\ . \tag{9}$$

It can be noted that if τ_r did not depend on temperature the two expressions (7) and (9) would be identical. However, if there were some dependence of τ_r on T it is clear that (9) would be much more likely to show it, since in (7) one might expect it to be suppressed by much stronger dependence on T coming from the $\exp(-E/kT)$ term. In this way the difference between temperature dependences of I and τ_{tot} observed by us can be rationalized as a result of additional temperature dependence of τ_r. There are three likely sources for change of radiative lifetime with temperature.

(a) An increase of the radiative transition rate due to the odd vibrations which make the symmetry-forbidden electronic transition more probable (Ballhausen-Liehr model). In the simplest case this is supposed to obey the $\coth(\hbar\omega_{odd}/2kT)$.

(b) A change in the effective radiative lifetime due to the population weighting of the doublet and quartet lifetimes, expressed by[27]

$$\frac{1}{\tau_{eff}}=\frac{\dfrac{1}{\tau(^2E)}+\dfrac{1}{\tau(^4T_2)}\exp(-d/kT)}{1+3\exp(-d/kT)}\ , \tag{10}$$

where $\tau(^2E)$ and $\tau(^4T_2)$ are the radiative lifetimes of the doublet and quartet, respectively. This may represent an increase or decrease of τ_{eff} with the temperature, depending on the sign of d.

(c) A change in the effective radiative lifetime due to the population weighting of the lifetimes of split components of the $^4T_2$.

We have found it difficult to reconcile the observed differences between the decay curve and the integrated intensity curve (Fig. 3) with (a). According to this mechanism the discrepancy between I and τ_{tot} should increase with temperature. However, for temperatures higher than 300 K the opposite is observed. Similarly mechanism (b) does not appear to play a major role. Since we presume $d<0$, one would expect an increase of the observed decay time with temperature, which is contrary to observation. If for some reason our interpretation of the 694-nm line was in error and d was larger than 0 (high-field case), then one would expect a much stronger decrease of τ_{eff} starting from much higher values characteristic of the doublet, which again is not the case. Thus we are left with mechanism (c) as the probable cause of the change of radiative lifetime with temperature. Although (c) qualitatively explains the experiment (weak temperature dependence of radiative lifetime for low temperatures and its saturation for higher temperatures) we do not have enough data to support this quantitatively. A similar situation was encountered by Payne *et al.* in MgF_2:Cr^{3+}.[28] Thus we tentatively assume that the 260-μs decay time observed at low temperature is the radiative lifetime of the dominant, low-energy component of the quartet state, which, for higher temperatures is averaged over all quartet components and eventually quenched by a nonradiative process.

C. Single-coordinate-configuration model

The data presented in the preceding section along with conclusions reached so far, enable us to construct a preliminary model of the Cr^{3+} luminescent center in sillimanite as shown in Fig. 7 and compare its predictions

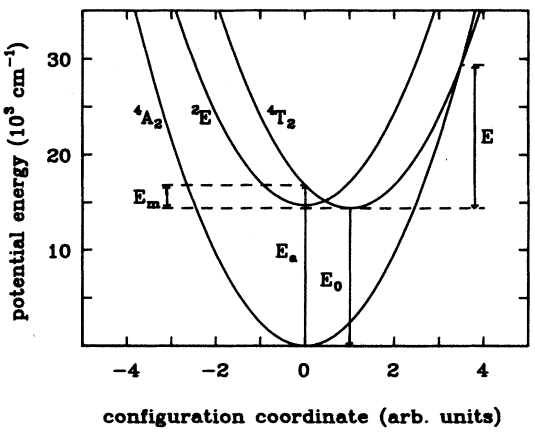

FIG. 7. Single-configuration-coordinate model of Cr^{3+} luminescence centrum in sillimanite. E, energy barrier for nonradiative transition; E_m, excess strain energy in the excited electronic state; E_0, zero-phonon energy; E_a, energy of absorption peak. The energy of the ^2E state was assumed to be 14 709 cm^{-1}.

TABLE II. Summary of nonradiative transition parameters for low-field, Cr-doped materials.

Host	Trans. rate[a] (s^{-1}), 300 K	E[b] (cm^{-1})	Frequency factor (s^{-1}) Experiment	Theory	References
Cs_2NaYCl_6	4.3×10^4	3810	3.7×10^{12}	0.33×10^{15}	5,4
	5.4×10^4	4250	3.8×10^{13}		16,4
K_2NaGaF_6	2.9×10^{-6}	9240	5.2×10^{13}	1.49×10^{15}	16,4
K_2NaScF_6	8.7×10^{-3}	7270	1.2×10^{13}	1.04×10^{15}	16,4
Ruby	1.2×10^4	4000	2.6×10^{12}		29
Sillimanite	1.04×10^3	1700	3.6×10^6	??	this paper

[a]Nonradiative transition rates at room temperature were calculated from experimental values of E and s.

[b]Energy barrier E is an experimental value.

with experiment. This model assumes linear coupling to one a_{1g} mode (340 cm^{-1}). Since[2]

$$E=\frac{(E_0-E_m)^2}{4E_m}\ ,\qquad E_m=E_a-E_0\ , \tag{11}$$

where E is the energy barrier between the excited and ground electronic states ($^4T_2$ and $^4A_2$), E_0 stands for the zero-phonon energy, E_a for energy of absorption peak, and E_m is an excess strain energy in the excited electronic state as shown in Fig. 7. E_m can be obtained from the emission spectrum assuming symmetry between emission and absorption bands (linear coupling). Taking $E_0=14\,409$ cm^{-1}, we find $E_m=2409$ cm^{-1} and $E=14\,940$ cm^{-1}. This value is much higher than the value found from the temperature quenching of the total intensity (1700 cm^{-1}). This result is hardly surprising in view of the previous results.[16] We see here yet another example of the inadequacy of the simple theory with just one, linearly coupled mode. However, since the 340-cm^{-1} mode-coupling coefficient is not much smaller than the total coupling coefficient found from the luminescence spectrum, we believe that anharmonicity or nonlinear coupling has to be introduced to the theory in order to reach agreement with experiment.[30,4]

D. Nonradiative transitions

Nonradiative processes in strongly lattice-coupled systems are often described by the simple Mott-Seitz theory.[31] It states that

$$\frac{1}{\tau_{nr}}=s\exp(-E/kT)\ , \tag{12}$$

where E is an energy barrier in a single-configuration-coordinate model and s is a frequency factor. Yet this theory, although descriptive of the temperature dependence, has been discredited on many occasions, sometimes explicitly,[16] sometimes implicitly.[32] The fact is, that often including the present case, the energy barrier derived from the construction of a configuration-coordinate diagram assuming linear coupling to a single mode is much larger than the experimental barrier, obtained by fitting [Eq. (1)]. This leads to discrepancies between observed and calculated rates which can reach several orders of magnitude.[16] There used to be a controversy about the frequency factor s expressing the matrix element for nonradiative transition from the electronic excited state to the electronic ground state. Since it has to involve promoting vibrational mode of appropriate symmetry, Andrews *et al.*[3] have argued that a vibrational deficiency in the high-symmetry environment of the Cr^{3+} ion can effectively produce a selection rule and hence slow down nonradiative rates. The role of symmetry selection rules was settled by Bartram *et al.*,[4] who calculated a generic promoting mode matrix element which leads to a frequency factor of approximately 10^{15}. This was based on universal presence of the t_{1g} promoting mode in all solids due to the hindered rotation of the oxygens around Cr. However, the frequency factor we have found is 9 orders of magnitude smaller and this poses a new theoretical challenge. It also stresses the importance of extracting both energy barrier and frequency factor from the experimental data. Data gathered in Table II unequivocally show that similar nonradiative transition rates can arise from different combinations of barriers heights and frequency factors. Large values of the energy barrier can effectively compensate for relatively large values of s, whereas for small barriers the nonradiative rates can be quite high even for genuinely small frequency factors. The present case tends to indicate the existence of a low-probability process (small promoting mode matrix element) coupled with a low barrier. Since the promoting mode would have to be different than t_{1g} the consequences of the departure from strictly octahedral symmetry for both promoting and accepting modes would have to be examined.

V. CONCLUSIONS

The broadband Cr^{3+} luminescence in sillimanite exhibits an interesting combination of features, for both basic (nonradiative transitions) and practical (solid-state tunable lasers) reasons. This includes long decay times, thermal stimulation of radiative rates, and relatively slow nonradiative rates. Some of these features, like the life-

time, can be rationalized in terms of the inversion symmetry of the Cr site. The simple, one-configuration-coordinate model was shown to fail to reproduce the observed energy barrier. The importance of separating the various terms determining nonradiative transition rates was demonstrated.

ACKNOWLEDGMENTS

We are grateful to P. Dunn of Museum of Natural History, Smithsonian Institution, who kindly provided us with the sample of sillimanite used in the course of this work, to F. Pink of GTE Laboratories Waltham, MA, for performing x-ray luminescence analysis, to Professor R. H. Bartram for invaluable discussions and suggestions, and to Dr. R. Angel of the Carnegie Institution of Washington for providing us with many illuminating comments on crystallography of mullite and aluminosilicates. The support of the U.S. Army Research Office under Grant No. DAAL03-86-0016 is also gratefully acknowledged.

*On leave from Institute of Physics, Nicholas Copernicus University, PL-87-100 Toruń, Poland.

[1]D. J. Robbins and A. J. Thomson, Philos. Mag. **36**, 999 (1977).
[2]A. M. Stoneham, Philos. Mag. **36**, 983 (1977).
[3]L. J. Andrews, A. Lempicki, and B. C. McCollum, Chem. Phys. Lett. **74**, 404 (1980).
[4]R. H. Bartram, J. C. Charpie, L. J. Andrews, and A. Lempicki, Phys. Rev. B **34**, 2741 (1986).
[5]R. Knochenmuss, Ch. Reber, M. V. Rajasekharan, and H. U. Gudel, J. Chem. Phys. **85**, 4290 (1986).
[6]L. J. Andrews, G. H. Beall, and A. Lempicki, J. Lumin. **36**, 65 (1986).
[7]A. J. Wojtowicz and A. Lempicki, J. Lumin. **39**, 189 (1988).
[8]S. O. Agrell and J. V. Smith, J. Am. Ceram. Soc. **43**, 69 (1960).
[9]R. Sadanaga, M. Tokonami, and Y. Takeuchi, Acta Crystallogr. **65**, 65 (1962).
[10]J. R. Smith and D. L. Bish, *Crystal Structures and Cation Sites of the Rock-Forming Minerals* (Allen and Unwin, Boston, 1987); P. H. Ribbe, in *Orthosilicates,* in Vol. 5 of *Review in Mineralogy* (Mineralogy Society of America, Washington, D.C., 1980); J. K. Winter and S. Ghose, Amer. Minerologist. **64**, 573 (1979).
[11]The analysis was performed by F. Pink of GTE Laboratories, Waltham, Massachusetts.
[12]P. T. Kenyon, L. Andrews, B. McCollum, and A. Lempicki, IEEE J. Quantum Electron. **QE-18**, 1189 (1982).
[13]N. T. Melamed, P. J. Viccaro, J. O. Artman, and F. de S. Barros, J. Lumin. **1/2**, 348 (1970).
[14]D. T. Palumbo, J. Lumin. **4**, 89 (1971).
[15]F. Bantien, P. Albers, and G. Huber, J. Lumin. **36**, 363 (1987).
[16]L. J. Andrews, A. Lempicki, B. C. McCollum, C. J. Giunta, R. H. Bartram, and J. F. Dolan, Phys. Rev. B **34**, 2735 (1986).
[17]S. T. Lai, B. H. T. Chai, M. Long, and R. C. Morris, IEEE J. Quantum Electron. **QE-22**, 1931 (1986).
[18]S. T. Lai, B. H. T. Chai, M. Long, M. D. Shinn, J. A. Caird, J. E. Marion, and P. R. Staver, in *Tunable Solid-State Lasers II,* edited by A. B. Budgor, L. Esterowitz, and L. G. DeShazer (Springer-Verlag, Berlin, 1986), Vol. 2, p. 145.
[19]A. D. Liehr and C. J. Ballhausen, Phys. Rev. **106**, 1161 (1957); L. L. Lohr, J. Chem. Phys. **50**, 4596 (1969).
[20]M. Lax, J. Chem. Phys. **20**, 1752 (1952).
[21]A. J. Wojtowicz and Cz. Koepke, Acta Physica Pol. A **71**, 385 (1987).
[22]L. J. Andrews, A. Lempicki, and B. C. McCollum, J. Chem. Phys. **74**, 5526 (1981).
[23]B. Struve and G. Huber, J. Appl. Phys. **57**, 45 (1985); K. Petermann and G. Huber, J. Lumin. **31/32**, 71 (1984).
[24]S. T. Lai, B. H. T. Chai, and M. Long, *Topical Meeting on Tunable Solid State Lasers Technical Digest Series, 1987* (Optical Society of America, Washington, D.C., 1987), Vol. 20, PD1, pp. 1–4.
[25]N. F. Mott and R. W. Gurney, *Electronic Processes in Ionic Crystals* (Oxford University Press, Oxford, England, 1948).
[26]C. C. Klick and J. H. Schulman, in *Solid State Physics,* edited by F. Seitz and D. Turnbull (Academic, New York, 1957), Vol. 5, pp. 97.
[27]P. Kisliuk and C. A. Moore, Phys. Rev. **160**, 307 (1967); B. Di Bartolo, *Optical Interaction in Solids* (Wiley, New York, 1968), p. 442.
[28]S. A. Payne, L. L. Chase, and W. F. Krupke, J. Chem. Phys. **86**, 3455 (1987).
[29]A. Misu, J. Phys. Soc. Jpn. **19**, 2260 (1964).
[30]M. D. Sturge, Phys. Rev. B **8**, 6 (1973).
[31]F. A. Kroger, *Some Aspects of the Luminescence of Solids* (Elsevier, New York, 1948).
[32]Ch. E. Byvik and A. M. Buonocristiani, IEEE J. Quantum Electron. **QE-21**, 1619 (1985).